Carbohydrate Polymers xxx (xxxx) xxx–xxx

Contents lists available at ScienceDirect

Carbohydrate Polymers

journal homepage: www.elsevier.com/locate/carbpol

Ultrasound assisted polyacrylamide grafting on nano-fibrillated cellulose

Haleh Sanaeishoar[a], Maryam Sabbaghan[b], Dimitris S. Argyropoulos[c,*]

[a] Department of Chemistry, Ahvaz Branch, Islamic Azad University, Ahvaz, Iran
[b] Chemistry Department, Faculty of Sciences, Shahid Rajaee Teacher Training University, PO Box 16785 163 Tehran, Iran
[c] Department of Forest Biomaterials, Organic Chemistry of Wood Components Laboratory, North Carolina State University, 2820 Faucette Drive, Raleigh, NC 27695-8005, United States

ARTICLE INFO

Keywords:
Nanofibrillated cellulose
Polyacryamide
Polyacrylamide grafted nanofibrillated cellulose
Graft copolymerization
Ultrasound
Intrinsic viscosity

ABSTRACT

Polyacrylamide has been grafted onto nanofibrillated cellulose (NFC-g-PAM) under mild conditions. This was accomplished by developing and optimizing an ultrasound assisted protocol in the presence of potassium persulfate initiator. The synthesis was optimized on the basis of maximizing grafting percentage and grafting efficiency by varying the initiator and monomer concentration. The data shows that ultrasound has a profound effect in promoting the grafting of PAM onto NFC. The intended grafting was confirmed and the properties of the new co-polymers were examined by elemental analyses, Fourier transform infrared spectroscopy, thermogravimetric analysis (TGA), and scanning electron microscopy (SEM). Intrinsic viscosity determinations in 0.1 M cupriethylenediamine solutions for the NFC-g-PAM copolymers and the starting NFC and PAM homopolymer revealed that grafting of PAM onto nanofibrillated cellulose has a profound effect on the hydrodynamic characteristics of the graft polymers.

1. Introduction

Turbak et al. and Herrick et al. first introduced nano-fibrillated cellulose (NFC) using wood pulp in a homogenizer, in 1983. The process promotes the exposure of cellulosic fibers into sub-structural fibrils and microfibrils. The typical length of NFC is several micrometers with a diameter less than 100 nm (Herrick, Casebier, Hamilton, & Sandberg, 1983; Turbak, Snyder, & Sandberg, 1983). Unlike cellulose nanocrystals, NFCs present a web like structure and exhibit both crystalline and amorphous domains. As anticipated, these materials show an extreme hydrogen bonding tendency, they are characterized by extremely high specific area and their aspect ratio, leads to extensive entanglement (Missoum, Belgacem, & Bras, 2013). There are three different terms in use today for describing NFC. These are: nanofibrillar cellulose (Ahola, Osterberg, & Laine, 2008; Stenstad, Andersen, Tanem, & Stenius, 2008), cellulose nanofiber (Abe, Iwamoto, & Yano, 2007) and cellulose nanofibril (Henriksson et al., 2007). The surface functionalized NFCs could be utilized in advanced material applications, including nanocomposites, separation membranes and nanoscale electronic devices (Li and Xia, 2004; Stenstad et al., 2008).

Both physical and chemical properties of natural and synthetic polymers can be altered by graft copolymerization with tangible practical implications. For example graft copolymerization of carboxymethyl cellulose (CMC) with polyacrylamide has been demonstrated to increase its viscosity and thermal stability (Biswal & Singh, 2004) being one of many examples. Surface graft copolymerization is known to affect the chemical properties of a polymer with significant material science ramifications. Overall, there are two classes of grafting methods: “grafting to” and “grafting from” (Ruckenstein & Li, 2005). “Grafting to” a surface of a polymeric substrate, involves the covalent and/or physical attachment of a preformed polymer with a distinct functionality, to reactive sites on the surface of the polymer substrate. In comparison, “grafting from” is initiated from the substrate’s surface, with a new polymer layer being created, by the successive addition of multiple monomer units via chain propagation from the initiating sites present on the surface of the substrate. The diffusion of small monomeric units in the “grafting from” approach offers considerable lower steric restrictions and phase differences imposed by the approaching monomer on the polymer substrate. Therefore, the “grafting from” approach is presumed to offer higher grafting efficiency compared to the “grafting to” approach (Roy, Semsarilar, Guthrie, & Perrier, 2009; Tizzotti, Charlot, Fleury, Stenzel, & Bernard, 2010).

Ultrasound waves of frequencies greater than 20 kHz have been described as a convenient and “green” way to promote chemical operations and organic transformations (Chowdhury & Viraraghavan, 2009; Lifka, Ondruschka, & Hofmann, 2003; Mason & Luche, 1997; Pingret, Fabiano-Tixier, & Chemat, 2013). Many investigators have demonstrated the advantages of using ultrasound waves in chemistry

* Corresponding author.
E-mail addresses: hsanaei@iauahvaz.ac.ir (H. Sanaeishoar), sabbaghan@srttu.edu (M. Sabbaghan), dsargyro@ncsu.edu (D.S. Argyropoulos).

https://doi.org/10.1016/j.carbpol.2017.11.042
Received 21 September 2017; Received in revised form 12 November 2017; Accepted 14 November 2017

since good yields, short reaction times, clean, selective and mild reactions are apparent in their presence (Gaplovsky, Gaplovsky, Toma, & Luche, 2000; Mason & Luche, 1997; Namboodiri & Varma, 2002; Zhang, Jin, Xie, Wu, & Wu, 2014). As anticipated, their utility in synthetic (Sadeghzadeh, Morsali, & Retailleau, 2010) and natural polymer synthesis (Klein, de Lima, da Feira, Brandalise, & de Camargo Forte, 2016) and modification efforts was immediately applied (Chu, Wei, & Zhu, 2015; Sackmann et al., 2015). The specific effects of ultrasound waves in the area of polymer synthesis include, generation of free radicals, activation of free radical initiators, homogenization of heterogeneous systems, degradation of polymers to produce macroradicals and dispersion of monomers to form heterogeneous particles (Chu et al., 2015; Paulusse & Sijbesma, 2006).

However, it is also possible to modify the polymer surface by graft copolymerization by utilizing free radicals. To this effect, several studies have been reported on NFC and recently reviewed (Missoum et al., 2013). For instance, Stentad et al. reported that grafted glycidyl methacrylate on NFC surfaces by cerium ammonium nitrate at 35 °C for 1 h in order to introduce vinyl groups on the surface of NFC. They showed that by such modification reaction it is possible to prepare NFCs with surfaces carrying substantial amounts of epoxy groups, carbon–-carbon double bonds, cationic groups (amines) and anionic groups (carboxylates anions). Furthermore Stenstad et al. (2008) have also demonstrated the possibility for rendering the NFC hydrophobic by grafting polymer brushes and layers. Littunen et al. (2011) described graft copolymerization of NFC with acrylic monomers using cerium ammonium nitrate as initiator at 35 °C for at least 1 h. All modifications imparted to NFC a more hydrophobic character with some improving its heat resistance. Maatar and Boufi (2015) demonstrated a poly(methacrylic acid-co-maleic acid) grafted nanofibrillated cellulose (NFC-MAA-MA) aerogel that was prepared via radical polymerization in an aqueous solution using Fenton's reagent at 50 °C for 2 h so as to promote its cationic adsorption character.

Overall, there has been no effort in the literature that reports the use of ultrasound energy in promoting graft copolymerization on NFC fibers. We thus commenced an investigation in this realm so as to enhance our understanding of such conditions. Our specific aim was to examine the efficacy of using the concerted action of a persulfate initiator with ultrasound in promoting the "grafting from" of polyacrylamide onto a commercial grade NFC and subsequent evaluation of the ensuing product characteristics.

2. Experimental

2.1. Materials

Nano Fibrillated Cellulose was provided by Stora Enso Corporation in the form of a gelatinous material containing approximately 5% by weight of solid polysaccharide. Acrylamide (AM) and potassium persulfate (KPS) were supplied by Merck Corporation and were used as received.

2.2. Graft polymerization

In a 100-mL three necked round-bottom flask, 10 g of NFC gel containing precisely 95% water (3 mmol of dry NFC) was diluted with 10 mL of distilled water and stirred for about 30 min. Catalytic amounts (as specified in Table 1) of a water soluble initiator, potassium persulfate $K_2S_2O_8$ (KPS), were then added as a solid and stirred for 15 min. An ultrasound probe (Omni-Ruptor 250 W) was then immersed into the reaction flask, via a rubber septum and flushed with nitrogen gas for 20 min. During the irradiation (at 50% power and at a frequency of 40 kHz and 15 min), the temperature of the reaction mixture rose to 70 °C using an oil bath (Table 1) and acrylamide monomer in 10 mL distilled water was gradually added over a period of 15 min for reaching the gel point. The gel like mass was poured into excess of acetone. The resulting precipitate was collected and dried in an oven set at 70 °C for 12 h. The dried precipitate was pulverized and purified by Soxhlet solvent extraction using DMF and acetic acid (1:1 v/v) for 12 h to remove the homopolymer. After washing the resulting copolymer by centrifugation for 10 min at 3000 rpm for three times with ethanol and finally water for three times, the grafted NFC was dried in a vacuum oven set at 70 °C for 24 h.

Table 1
Synthesis details of graft copolymers.

Sample Identity	Mole Ratio AM/NFC	Mole Ratio KPS/NFC	% G[1]	% E[2]
NFC-g-PAM 1	10: 1	0.06: 1	258	68
NFC-g-PAM 2	13: 1	0.06: 1	357	69
NFC-g-PAM 3	16: 1	0.06: 1	347	57
NFC-g-PAM 4	13: 1	0.09: 1	508	93
NFC-g-PAM 5	13: 1	0.03: 1	286	59
Control reaction A[3]	13: 1	0.06: 1	120	34
Control reaction B[4]	13: 1	0.06: 1	211	47
Control reaction C[5]	13: 1	0.06: 1	–	–
Control reaction D[6]	13: 1	0.06: 1	153	39
Control reaction E[7]	13: 1	0.06: 1	149	38

[1] Grafting percentage.
[2] Grafting efficiency.
[3] Polymer obtained as per conditions for NFC-g-PAM 2 in the absence of heat.
[4] Polymer obtained as per conditions for NFC-g-PAM 2 in the absence of ultrasound.
[5] Polymer obtained as per conditions for NFC-g-PAM 2 in the absence of heat and ultrasound.
[6] Polymer obtained as per conditions for NFC-g-PAM 2. The NFC and KPS mixture was brought to 70 °C followed by sonication and acrylamide gradual addition over a period of 15 min.
[7] Polymer obtained as per conditions for NFC-g-PAM 2. KPS was added under nitrogen after the NFC was heated to 70 °C followed by sonication and acrylamide gradual addition over a period of 15 min.

Polyacrylamide (PAM) polymer was synthesized as control, using identical conditions to those of the graft reaction 0.185 mmol of initiator and a monomer concentration of 3 M but without the addition in the absence of NFC.

Control reactions A, B, C, D and E were carried under the reaction conditions described in Table 1 for NFC-g-PAM 2. Control reaction A was carried out in the absence of heat while control reaction B was carried out in the absence of ultrasound and control reaction C was carried in the absence of both heat and ultrasound. For control reaction D, once the mixture of NFC and KPS was prepared (under nitrogen), it was brought to 70° using an oil bath. Once temperature was reached, the sonication commenced and acrylamide (dissolved in 10 mL of water) was gradually added over a period of 15 min, after which the gel point was attained. Finally for control reaction E, the KPS was added under nitrogen to NFC heated to 70 °C and then was sonicated and acrylamide (dissolved in 10 mL water) was gradually added over a period of 15 min, after which the gel point was attained.

The grafting percentage (% G) and grafting efficiency (% E) were calculated according to Toti and Aminabhavi (2004):

$$\%\ \text{Grafting percentage}\ (\%G) = \frac{\text{wt. of graft copolymer} - \text{wt. of NFC}}{\text{wt. of NFC}} \times 100$$

$$\%\ \text{Grafting efficiency}\ (\%E) = \frac{\text{wt. of graft copolymer}}{\text{wt. of NFC} + \text{wt. of acrylamide monomer}} \times 100$$

2.3. Product characterization

2.3.1. Elemental analyses

Elemental analyses of the starting material NFC and the graft copolymers were performed using a Perkin Elmer CHN 2400 series II

CHNO/S Elemental Analyzer (Waltham, MA); Table 2 tabulates the obtained data.

2.3.2. Intrinsic viscosity

The relative viscosity of all samples was determined using a capillary Ubbelohde viscometer with a constant: 0.004 $mm^2 s^{-1}$. The viscosities were measured in a 0.1 M cupriethylenediamine (CED) solution at 25.0 ± 0.1 °C. The flow time for all solutions was measured at three different concentrations attained via dilution. More specifically 0.05, 0.025, 0.0125 g of samples were mixed with 5 mL of distilled water and then 5 mL of cupriethylenediamine solution in a stomacher bag and homogenized for several minutes using a stomacher (Lab. Blender 80, Seward Medical, London, UK). The ratio of the time of flow of the polymer solution (t) and that of the solvent (t_0), offered the relative viscosity ($\eta_{rel} = t/t_0$). The specific viscosity was then calculated from the relation $\eta_{sp} = \eta_{rel}$-1. The intrinsic viscosity was obtained by extrapolation of the η_{sp}/c versus c plot to zero concentration (Adhikary, Krishnamoorthi, & Singh, 2011). All polymer concentrations were expressed as g/dL and the final intrinsic viscosities expressed as dL/g (Table 3).

2.3.3. FT-IR spectroscopy

The IR spectra of NFC, PAM, and the graft copolymers were recorded in the solid state and measured on a Thermo Nicolet NEXUS 670 FT-IR infrared spectrophotometer. Spectra in the range of 650–4000 cm^{-1} were obtained with a resolution of 4 cm^{-1}.

2.3.4. Thermogravimetric analysis

Such thermograms were acquired using a TA TGA-Q500 instrument. Approximately 6–10 mg of the polymer were used to determine its mass loss during heating up to 600 °C at a heating rate of 10 °C/min. The samples were purged with nitrogen at a flow rate of 50 mL/min. The balance's purge gas (nitrogen) was set at a flow rate of 40–50 mL/min during the thermogram acquisition.

2.3.5. Field-emission scanning electron microscopy (FE-SEM)

The morphologies of the blends were examined using an FEI Verios 460L SEM to collect the data. The electron beam had energy of 1 keV with a current of 50 pA and a stage bias of 500 V. The Verios allows for high resolution (0.7 nm is achievable at 1 kV) at low voltages.

3. Results and discussion

3.1. Grafting mechanism

Our current knowledge about the mechanism of acrylamide grafting onto cellulosic substrates and by extension to NFC is shown in Scheme 1 (Berlin & Kislenko, 1992; Mahdavinia, Pourjavadi, Hosseinzadeh, & Zohuriaan, 2004). The synergistic effect between the persulfate initiator and the ultrasound energy facilitates the formation of sulfate ion radicals. A hydrogen abstraction from the hydroxyl groups of the polysaccharide to form an alkoxy radical on the substrate then occurs (sequence (**i**), Scheme 1). Overall, these two reactions involve the initiation phase of the co-polymerization chemistry. In the propagation step (**ii**), or single unit of acrylamide monomer is added on the NFC backbone ($\mathbf{ii})_{\mathbf{a}}$, then more acrylamide monomers are attached on the NFC backbone through acrylamide chains and the length of the grafted chains increases ($\mathbf{ii})_{\mathbf{b}}$. In the termination step (**iii**), two growing chains are coupled together thus terminating any subsequent chain growth events.

3.2. Grafting reaction

Table 1 shows the persulfate initiated, ultrasound assisted synthesis details of the graft copolymers (NFC-g-PAM) of polyacrylamide on NFC.

Our initial efforts focused at optimizing the reaction conditions. For this purpose, two series of graft copolymers (a total of five NFC-g-PAM 1-5) were synthesized by varying the concentrations of KPS and acrylamide (AM). During the series (NFC-g-PAM 1-3), the amounts of NFC and KPS were kept constant while the amount of acrylamide used was systematically varied. Increasing of monomer concentration had a minor effect on increasing the percentage of grafting and the grafting efficiency. It seems that beyond a certain threshold and at higher monomer concentrations the primary radicals promote the self-polymerization of the AM monomer instead of reacting with the backbone substrate NFC polymer. Earlier efforts showed using carboxymethylated chitosan (Joshi & Sinha, 2007) that once the graft copolymer radical has formed, excess monomer may shield the graft copolymer, inhibiting further grafting. Furthermore, excess monomer may also consume available initiator radicals initiating homopolymerization with a concomitant decrease in % G.

During the second series of our optimization experiments (NFC-g-PAM 2, 4, 5), the amounts of NFC and AM were kept constant, while the KPS concentration was varied. Since the concentration of acrylamide was constant, in this series, the% G and% E was found to increase with an increase in the initiator concentration and reached a maximum for NFC-g-PAM 4 with a determined% G and% E of 508 and 93 respectively. This is probably due to KPS directly attacking and abstracting hydrogen from within the NFC backbone producing oxygen centered free radicals initiating PAM grafting onto it. During our work we observed that the formation of PAM homopolymer was considerably less at high initiator concentrations as indicated by the% G that approached 100% (actual value obtained was 93; Table 1) for NFC-g-PAM 4, where the highest KPS concentration was used.

The conditions for producing such high grafting efficiencies were thus considered as being the optimum conditions for subsequent investigations as tabulated for NFC-g-PAM 4 in Table 1.

In an effort to further understand and probe the significance of heat and ultrasonic energy applied, we carried out a series of control reactions by using beyond a certain threshold the conditions of NFC-g-PAM 2. A control reaction (A) was carried out in the absence of heat, while control reaction (B) was carried out at 70 °C in the absence of ultrasound energy and control reaction (C) was carried out in the absence of both heat and ultrasound. By comparing the grafting percentage (% G) obtained for NFC-g-PAM 2 with control reaction A, the significance of heat becomes apparent In addition, the positive effect of ultrasound is apparent when one compares the grafting percentage (% G) for NFC-g-PAM 2, where ultrasound was used to that of control reaction B, where no ultrasound was used. Furthermore, for the same reactions, the efficiency of hydrogen abstraction as demonstrated by% E was 69% in the presence of ultrasound and only 47% in its absence (Klein et al., 2016). An increase of 22% in the%E value and a decrease in the amount of homopolymer formation was apparent (from 53% to 31%) when ultrasound energy was used. Additional efforts described by control reactions D and E showed that minor effects were operational depending when the onset of heating commenced.

Our data so far indicates that ultrasound effectively promotes the grafting of PAM onto NFC via a heterogeneous reaction. It is likely that the ultrasound energy promotes radical generation and assists the creation of homogeneous conditions. Table 1, demonstrates that control reaction conditions C (carried out in the absence of heat and ultrasound) effectively offered no grafting.

3.3. Elemental analyses

The elemental analyses for NFC, PAM homopolymer and all graft copolymers synthesized are shown in Table 2. As anticipated NFC contains no nitrogen and the lowest percentages of carbon and hydrogen. The presence of nitrogen for all NFC-g-PAM copolymers demonstrates that PAM chains have in fact been grafted on the NFC backbone. Amongst the series of the graft copolymers synthesized, the nitrogen content for NFC-g-PAM 4 was shown to be the highest in

accordance with the measured %G and %E values of 508% and 93% respectively. This independently confirms the significance of high concentrations of initiator in promoting the sought reaction.

Table 2
Elemental analysis of NFC, PAM and graft copolymers.

Samples	% C	% H	% N
NFC	42.92	6.83	–
NFC-g-PAM 1	44.85	7.23	7.13
NFC-g-PAM 2	43.65	7.32	11.42
NFC-g-PAM 3	43.25	7.25	10.97
NFC-g-PAM 4	44.81	7.53	13.47
NFC-g-PAM 5	44.10	7.27	7.89
PAM	45.82	7.86	17.84

3.4. Determination of intrinsic viscosity

While the elemental analyses data presented in Table 2 offers a confirmation of grafting and a semi-quantitative indication of its magnitude amongst the various copolymers samples synthesized, indications of the actual length of the grafted PAM polymer chains on the NFC is unknown. Measuring the solution viscosity of the various copolymers synthesized was sought as a means of further delving into the details of the actual molecular length of the polymer chains attached on the NFC. This is because, once PAM is grafted on the NFC, the effective hydrodynamic volume of the resulting material in solution should offer alterations on the way the solutions flows through a narrow capillary. The intrinsic viscosities of NFC, PAM and all graft copolymers are reported in Table 3.

The NFC used in this study was determined to have an intrinsic viscosity of 0.09 dL/g while the PAM homopolymer synthesized showed an intrinsic viscosity of about thirty times higher. This indicates that the effective hydrodynamic radius of a PAM polymer molecule is most likely larger offering greater resistance to flow than any solvated NFC chain. This by itself is rather interesting since it qualitatively demonstrates that the NFC polymer chains may be significantly smaller than the PAM homopolymer. To further delve into this issue we also measured the intrinsic viscosity of fully bleached softwood pulp that had not been subjected to any intensive defibration process. The obtained value for it was: 0.67 dL/g. The fully bleached softwood pulp showed a number-average molecular weight (M_n) value of approximately 9 times higher than the NFC material used in our work. This by itself shows that the process of producing NFC dramatically reduces the actual Mn of the cellulose via likely mechano-chemically induced chain scission reactions.

Table 3
Intrinsic viscosity and number-average molecular weights for NFC, PAM and graft copolymers.

Sample	[η] (dL/g)	$M_n \times 10^5$
NFC	0.09	0.16 [1]
Fully bleached softwood pulp	0.67	1.4 [1]
NFC-g-PAM 1	1.07	21.74 [2]
NFC-g-PAM 2	1.75	45.69 [2]
NFC-g-PAM 3	1.98	55.06 [2]
NFC-g-PAM 4	2.25	66.78 [2]
NFC-g-PAM 5	1.55	38.04 [2]
PAM	2.63	84.53 [2]

[1] $[\eta] = 1.33 \times 10^{-4} (M_n)^{0.905}$, (Saxena, Bhatnagar, & Biswas, 1963).
[2] $[\eta] = 6.8 \times 10^{-4} (M_n)^{0.66}$, (Biswal & Singh, 2004).

Table 3 also displays the calculated number-average molecular weights (M_n) of the synthesized copolymer and polymer samples estimated from the intrinsic viscosity [η] values. For this purpose the Mark Houwink equation, ($[\eta] = KM^{\alpha}$) was employed (K and α values are constants specified for a particular polymer/solvent/temperature system). For PAM the values of K and α used were $[\eta] = 6.8 \times 10^{-4} (M_n)^{0.66}$ with M_n being the number-average molecular weight (Biswal & Singh, 2004).

Grafting PAM onto NFC has an immediate effect in the intrinsic viscosity even for samples that showed the lowest % grafting and grafting efficiency values. These large effects observed are additional

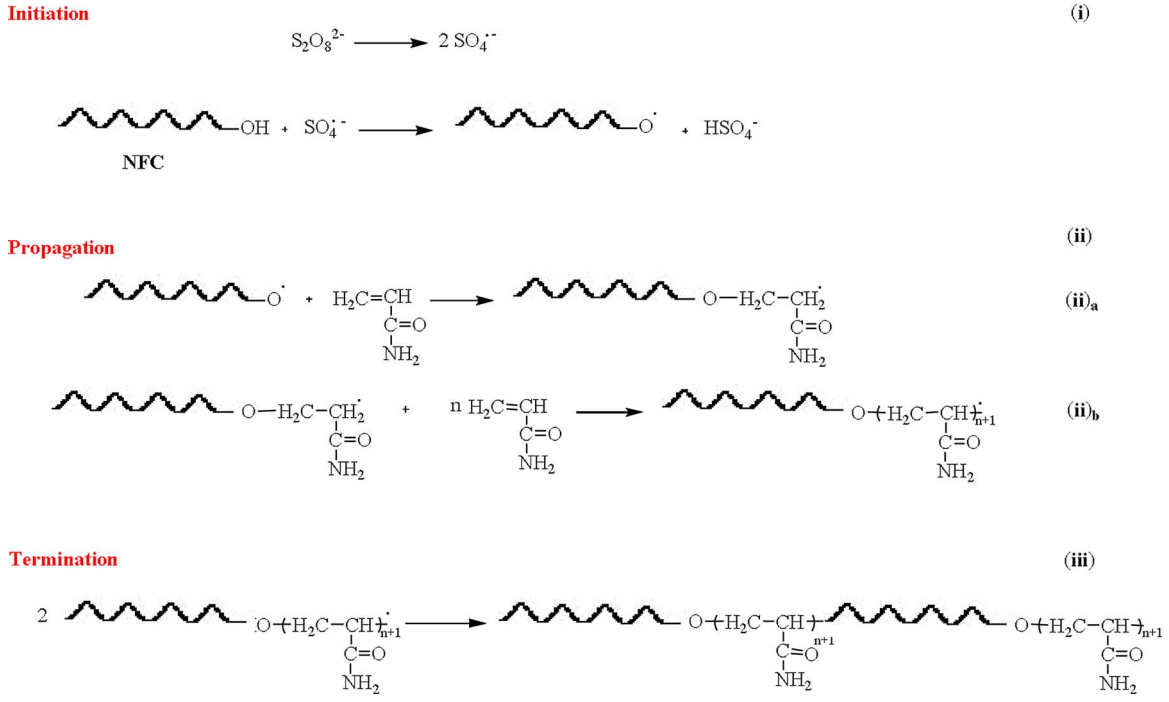

Scheme 1. Schematic representation for synthesis of NFC-g-PAM via an ultrasound assisted method.

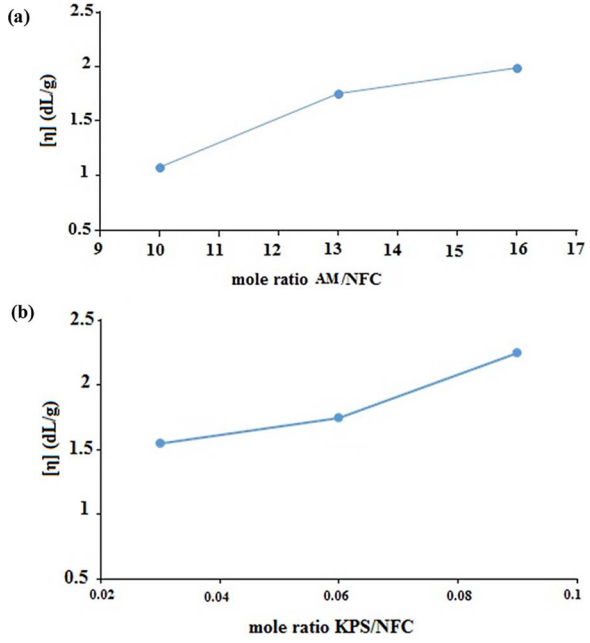

Fig. 1. (a) Effect of mole ratio AM/NFC on intrinsic viscosity, (b) Effect of mole ratio KPS/NFC on intrinsic viscosity.

independent indications of effective grafting of PAM onto NFC. All NFC graft copolymers obtained in the series NFC-g-PAM 1, and 3 show the effect of concentration of acrylamide on the intrinsic viscosity of the copolymer. An increase in the concentration of acrylamide shows concomitant intrinsic viscosity increases reaching a maximum with NFC-g-PAM 3. We consider these conditions as offering an optimum maximum PAM chain length as displayed by the highest intrinsic viscosity obtained (da Silva, de Paula, & Feitosa, 2007). This is further corroborated, in the series NFC-g-PAM 2, 4, 5, where the intrinsic viscosities (and by consequence the length of the NFC-g-PAM chains) are also seen to increase at higher initiator concentrations. Overall, higher initiator and monomer concentrations resulted in increases in intrinsic viscosity (Fig. 1a, b respectively). The intrinsic viscosity data obtained for NFC-g-PAM 4 shows that higher initiator concentrations are more effective in promoting grafting than higher monomer concentrations.

3.5. FT-IR spectroscopy

To further confirm the covalent grafting of PAM onto NFC the infrared spectra of NFC, PAM, and NFC-g-PAM 4 co-polymer were examined (Fig. 2). The initial unmodified NFC shows the anticipated hydrogen bonded OH stretching vibration at 2990–3700 cm^{-1}. Similarly, the CH stretching of it is apparent at 2894 cm^{-1} while the OH bending vibration for the adsorbed water is apparent at 1644 cm^{-1}. Additional assignments for various other vibrational modes were observed as follows; CH_2 bending (1428 cm^{-1}); CH bending (1369 cm^{-1} and 1317 cm^{-1}); C—O stretching (1041 and 1023 cm^{-1}); The CH bending or CH_2 stretching was also apparent at about 900 cm^{-1} which substantiates aspects of its amorphous structure (Lu, Askeland, & Drzal, 2008).

The PAM spectrum showed a broad band around 3342 cm^{-1} and a characteristic peak at 3215 cm^{-1} due to the stretching vibration of N—H. The significant characteristic peaks at 1651 and 1606 cm^{-1} were attributed to the carbonyl stretching vibration and N—H bending vibration of the amide group, respectively (Zhou & Wu, 2011). Meanwhile, the FT-IR spectrum of NFC-g-PAM 4 exhibits the strong absorption at 3340 cm^{-1} and the shoulder at around 3198 cm^{-1}. These are both attributed to N—H stretching. The sharp absorption peak at 1650 cm^{-1} and a shoulder at 1611 cm^{-1}, attributed to the C═O (primary amide) stretching and the NH_2 bending vibrations of PAM, respectively. Thus, the presence of these additional peaks in case of grafted NFC compared to that of NC confirms the successful grafting of PAM chains onto the backbone of NFC.

3.6. Thermogravimetric analysis

The actual thermal degradation profiles for NFC, PAM, and NFC-PAM 4 at the temperature range 30–600 °C under a nitrogen atmosphere was also examined by TGA analyses in Fig. 3. The derivatives of the weight loss were also selected to be displayed since this offered the discussed effects with more clarity.

At temperatures below 200 °C, an initial weight loss is apparent for NFC but it is a lot less than in the case of PAM and the copolymer. This could be the result of traces of bound water remaining within the structure of the NFC which is significantly removed in the case of the graft copolymer and of course absent from the homopolymer. At temperatures close to 250 °C, the decomposition of the unmodified NFC is shown to commence with a maximum at 330 °C, and its effective

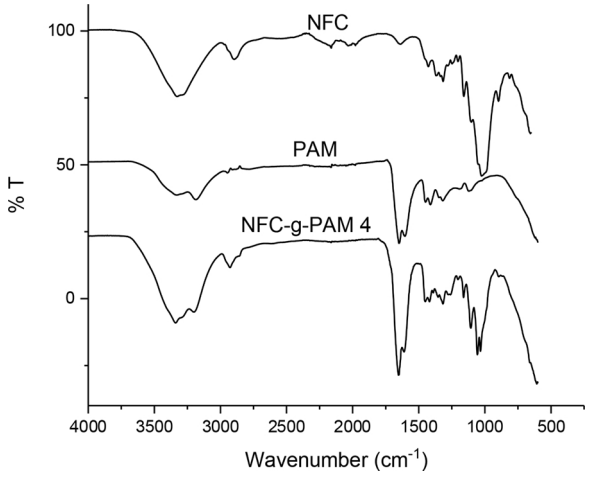

Fig. 2. Infrared spectra of NFC, PAM and NFC-g-PAM 4.

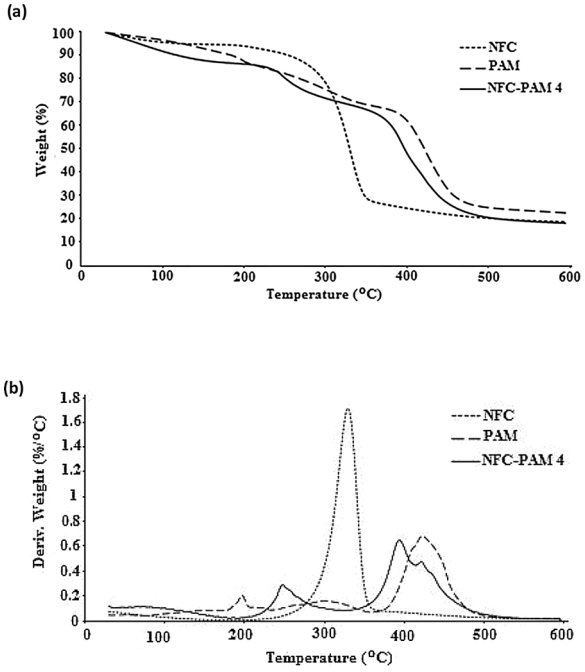

Fig. 3. (a) TGA and (b) DTG curves of NFC, PAM, NFC-g-PAM 4.

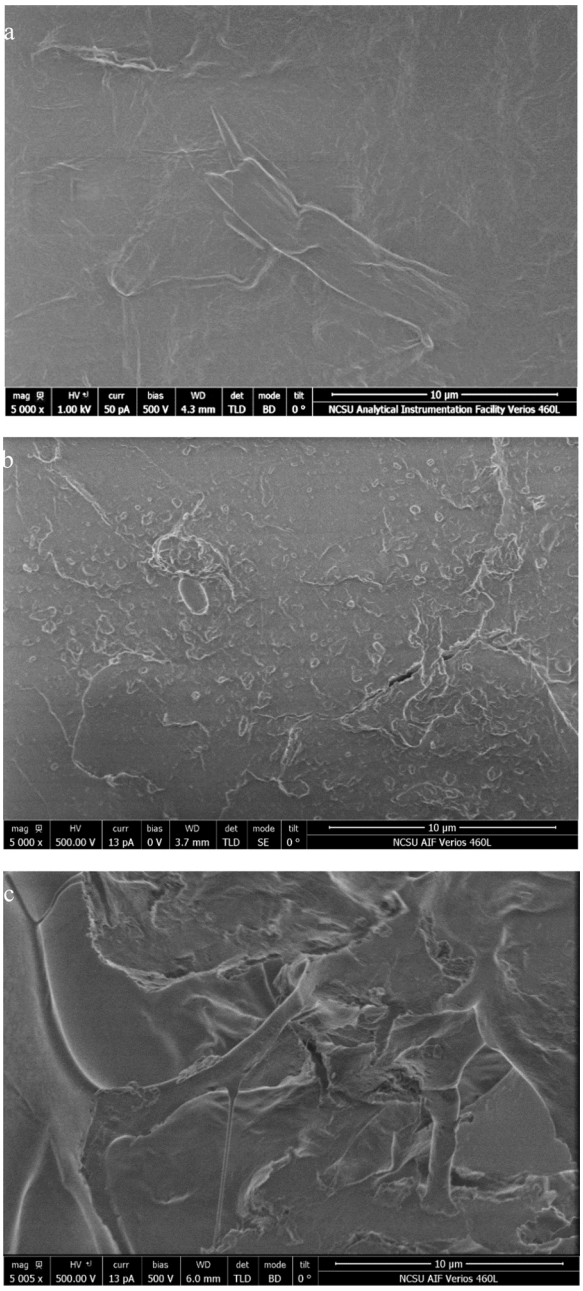

Fig. 4. SEM micrograph of (a) NFC, (b) PAM and (c) NFC-g-PAM 4.

complete degradation at around 360 °C (Littunen et al., 2011). PAM, however, is seen to decompose with maximum weight losses in three temperature regimes with maxima at 198 °C, 300 °C, and 425 °C (Fig. 3) The PAM degradation observed between 230 and 360 °C has been rationalized on the basis of a deamination reaction manifested by the loss of ammonia (Biswal & Singh, 2004).

In this context, the thermograms of Fig. 3a show that the deamination reaction is somewhat less effective (within the same temperature range) when NFC is grafted on PAM. At around 370 °C the third decomposition phase for PAM is seen to commence and extend to around 500 °C with the maximum decomposition temperature (T_{max}) about 425 °C. This is mostly the result of the PAM chains degradation (Zhou & Wu, 2011). The accumulated thermal degradation information for NFC and PAM allows one to arrive at the following conclusions.

The derivative data of Fig. 3b clearly demonstrates that the first two thermal decomposition events (250 °C, 395 °C) took place at temperatures greater than those for PAM (198 °C) and NFC (330 °C). Overall, the weight loss curves (Fig. 3a & b) shows that the thermal stability of the grafted NFC is an intermediate between unmodified NFC and PAM which emphasizes its "composite" character.

3.7. Scanning electron microscopy (SEM)

The surface morphologies of NFC, PAM and NFC-g-PAM 4 (selected for imaging) were examined via scanning electron microscopy (SEM) as shown in Fig. 4 (data displayed at the same magnification for comparison purposes).

While the initial NFC shows the anticipated fibrillary nature of the sample (Fig. 4a), this is not the case for the amorphous PAM (Fig. 4b). The morphology of the grafted NFC, as seen in Fig. 4c, is seen to be a composite picture of the individual NFC fibrils and PAM. The comparison of the micrographs clearly shows that the surface morphology of the NFC changes upon grafting fibers, indicating that a considerable amount of polyacrylamide has been grafted onto NFC (Thakur, Singha, & Thakur, 2012).Furthermore, the grafted copolymer showed a more rough surface most likely promoted by grafting of PAM onto it (Singh, Nath, & Guha, 2011).

4. Conclusions

Polyacrylamide grafted nanofibrillated cellulose has been successfully synthesized under mild aqueous conditions by the concerted action of ultrasound energy and chemical initiation. Effective grafting was obtained even at low acrylamide/NFC ratios. Although the heat and ultrasound both effected the efficiency of grafting, the effect of heat was found to be more notable. NFC-g-PAM copolymer containing a high degree of grafted PAM produced with good grafting efficiency was obtained using a molar ratio of AM to NFC of 13:1 and a mole ratio of KPS to NFC of 0.062: 1. All copolymers showed to possess intrinsic viscosity values considerably higher (about 25 times higher) than that of the starting NFC and close to that of the homo-polymer PAM synthesized. Such observations add further credibility to the fact that effective grafting of PAM chains of relatively high number-average molecular weight, was induced during the developed protocol. Thermagravimetric analyses (TGA) and morphological studies of the graft copolymers, NFC and PAM further supported our overall conclusions of effective grafting onto the gelatinous NFC substrate.

Acknowledgments

The authors gratefully acknowledge Stora Enso corporation for kindly providing a sample of Nano fibrillated cellulose used in this work. HS wish to thank the Ahvaz Branch, Islamic Azad University and MS gratefully acknowledge the Shahid Rajaee Teacher Training University, for providing the essential financial support for their visit to the Laboratories of professor Argyropoulos at NCSU.

References

Abe, K., Iwamoto, S., & Yano, H. (2007). Obtaining cellulose nanofibers with a uniform width of 15 nm from wood. *Biomacromolecules, 8*, 3276–3278.

Adhikary, P., Krishnamoorthi, S., & Singh, R. P. (2011). Synthesis and characterization of grafted carboxymethyl guar gum. *Journal of Applied Polymer Science, 120*, 2621–2626.

Ahola, S., Osterberg, M., & Laine, J. (2008). Cellulose nanofibrils-adsorption with poly (amideamine) epichlorohydrin studied by QCM-D and application as a paper strength additive. *Cellulose, 15*, 303–314.

Berlin, A. A., & Kislenko, V. N. (1992). Kinetics and mechanism of radical graft polymerization of monomers onto polysaccharides. *Progress in Polymer Science, 17*, 765–825.

Biswal, D. R., & Singh, R. P. (2004). Characterisation of carboxymethyl cellulose and polyacrylamide graft copolymer. *Carbohydrate Polymers, 57*, 379–387.

Chowdhury, P., & Viraraghavan, T. (2009). Sonochemical degradation of chlorinated organic compounds: Phenolic compounds and organic dyes – A review. *Science of the Total Environment, 407*, 2474–2492.

Chu, H.-G., Wei, H.-L., & Zhu, J. (2015). Ultrasound enhanced radical graft polymerization of starch and butyl acrylate. *Chemical Engineering and Processing, 90*, 1–5.

da Silva, D. A., de Paula, R. C. M., & Feitosa, J. P. A. (2007). Graft copolymerisation of

acrylamide onto cashew gum. *European Polymer Journal, 43*, 2620–2629.
Gaplovsky, A., Gaplovsky, M., Toma, S., & Luche, J. L. (2000). Ultrasound effects on the photopinacolization of benzophenone. *The Journal of Organic Chemistry, 65*, 8444–8447.
Henriksson, M., Henriksson, G., Berglund, L. A., & Lindstrom, T. (2007). An environmentally friendly method for enzyme assisted preparation of microfibrillated cellulose (MFC) nanofibers. *European Polymer Journal, 43*, 3434–3441.
Herrick, F. W., Casebier, R. L., Hamilton, J. K., & Sandberg, K. R. (1983). Microfibrillated cellulose; morphology and accessibility. *Journal of Applied Polymer Science, 37*, 797–813.
Joshi, J. M., & Sinha, V. K. (2007). Ceric ammonium nitrate induced grafting of polyacrylamide onto carboxymethyl chitosan. *Carbohydrate Polymers, 67*, 427–435.
Klein, J. M., de Lima, V. S., da Feira, J. M. C., Brandalise, R. N., & de Camargo Forte, M. M. (2016). Chemical modification of cashew gum with acrylamide using an ultrasound-assisted method. *Journal of Applied Polymer Science,* 133. http://dx.doi.org/10.1002/APP.43634.
Li, D., & Xia, Y. (2004). Electrospinning of nanofibres: Reinventing, the wheel? *Advanced Materilas, 16*, 1151–1170.
Lifka, J., Ondruschka, B., & Hofmann, J. (2003). The use of ultrasound for the degradation of pollutants in water: Aquasonolysis – A review. *Engineering in Life Sciences, 3*, 253–262.
Littunen, K., Hippi, U., Johansson, L., Österberg, M., Tammelin, T., Laine, J., et al. (2011). Free radical graft copolymerization of nanofibrillated cellulose with acrylic monomers. *Carbohydrate Polymers, 84*, 1039–1047.
Lu, J., Askeland, P., & Drzal, L. T. (2008). Surface modification of microfibrillated cellulose for epoxy composite application. *Polymer, 49*, 1285–1296.
Maatar, W., & Boufi, S. (2015). Poly(methacylic acid-co-maleic acid) grafted nanofibrillated cellulose as a reusable novel heavy metal ions adsorbent. *Carbohydrate Polymers, 126*, 199–207.
Mahdavinia, G. R., Pourjavadi, A., Hosseinzadeh, H., & Zohuriaan, M. J. (2004). Modified chitosan 4: Superabsorbent hydrogels from poly(acrylic acid-co-acrylamide) grafted chitosan with salt and pH-responsiveness properties. *European Polymer Journal, 40*, 1399–1407.
Mason, T. J., & Luche, J. L. (1997). In R. V. Eldick, & C. D. Hubbard (Eds.). *Chemistry under extreme or non-classical conditions*New York: Wiley [p. 317].
Missoum, K., Belgacem, M. N., & Bras, J. (2013). Nanofibrillated cellulose surface modification: A review. *Materials, 6*, 1745–1766.
Namboodiri, V. V., & Varma, R. S. (2002). Solvent-free sonochemical preparation of ionic liquids. *Organic Letter, 4*, 3161–3163.
Paulusse, J. M. J., & Sijbesma, R. P. (2006). Ultrasound in polymer chemistry: Revival of an established technique. *Journal of Polymer Science Part A, 44*(19), 5445–5453.
Pingret, D., Fabiano-Tixier, A.-S., & Chemat, F. (2013). Degradation during application of ultrasound in food processing: A review. *Food Control, 31*, 593–606.
Roy, D., Semsarilar, M., Guthrie, J. T., & Perrier, S. (2009). Cellulose modification by polymer grafting: A review. *Chemical Society Review, 38*, 2046–2064.
Ruckenstein, E., & Li, Z. F. (2005). Surface modification and functionalization through the self-assembled monolayer and graft polymerization. *Advances in Colloid and Interface Science, 113*, 43–63.
Sackmann, J., Burlage, K., Gerhardy, C., Memering, B., Liao, S., & Schomburg, W. K. (2015). Review on ultrasonic fabrication of polymer micro devices. *Ultrasonics, 56*, 189–200.
Sadeghzadeh, H., Morsali, A., & Retailleau, P. (2010). Ultrasonic-assisted synthesis of two new nano-structured 3D lead (II) coordination polymers: Precursors for preparation of PbO nano-structures. *Polyhedron, 29*, 925–933.
Saxena, V. P., Bhatnagar, H. L., & Biswas, A. B. (1963). Viscometric determination of molecular weight of cellulose pulps in zinc ethylenediamine solution. *Journal of Applied Polymer Science, 7*, 181–186.
Singh, A. V., Nath, L. K., & Guha, M. (2011). Microwave assisted synthesis and characterization of Sago starch-g-acrylamide. *Starch, 63*, 740–745.
Stenstad, P., Andresen, M., Tanem, B. S., & Stenius, P. (2008). Chemical surface modifications of microfibrillated cellulose. *Cellulose, 15*(1), 35–45.
Thakur, V. K., Singha, A. S., & Thakur, M. K. (2012). Rapid synthesis of MMA grafted pine needles using microwave radiation. *Polymer-Plastics Technology and Engineering, 51*, 1598–1604.
Tizzotti, M., Charlot, A., Fleury, E., Stenzel, M., & Bernard, J. (2010). Modification of polysaccharides through controlled/living radical polymerization grafting-towards the generation of high performance hybrids. *Macromolecular Rapid Communications, 31*, 1751–1772.
Toti, U. S., & Aminabhavi, T. M. (2004). Modified guar gum matrix tablet for controlled release of diltiazem hydrochloride. *Journal of Controlled Release, 95*, 567–577.
Turbak, A. F., Snyder, F. W., & Sandberg, K. R. (1983). Microfibrillated cellulose, a new cellulose product: Properties, uses, and commercial potential. *Journal of Applied Polymer Science, 37*, 815–827.
Zhang, L., Jin, Y., Xie, Y., Wu, X., & Wu, T. (2014). Releasing polysaccharide and protein from yeast cells by ultrasound: Selectivity and effects of processing parameters. *Ultrasonics Sonochemistry, 21*, 576–581.
Zhou, C., & Wu, Q. (2011). A novel polyacrylamide nanocomposite hydrogel reinforced with natural chitosan nanofibers. *Colloids and Surfaces B: Biointerfaces, 84*, 155–162.